Advances in Science and Technology Research Journal

Advances in Science and Technology Research Journal, 2025, 19(9), 369–384
https://doi.org/10.12913/22998624/207858
ISSN 2299-8624, License CC-BY 4.0

Received: 2025.06.27
Accepted: 2025.07.15
Published: 2025.08.01

Assessing electrode wear: The role of spot weld count in material degradation

Rafał Dziurka[1*], Dawid Stanisz[2], Sławomir Parzych[3], Wiktoria Zbyrad-Kołodziej[4], Monika Bochenek[2]

[1] Faculty of Metals Engineering and Industrial Computer Science, AGH University of Science and Technology, aleja A. Mickiewicza 30, 30-59 Krakow, Poland
[2] PRAXWELD Sp. z o.o., ul. Łącznik 21A, 33-300 Nowy Sącz, Poland
[3] Faculty of Materials Science and Physics, Cracow University of Technology, ul. Podchorążych 1, 30-084 Kraków, Poland
[4] Faculty of Mechanics and Technology, Rzeszów University of Technology, ul. Kwiatkowskiego 4, 37-450 Stalowa Wola, Poland
* Corresponding author's e-mail: dziurka@agh.edu.pl

ABSTRACT

This study investigates the degradation of electrodes during the resistance spot-welding process and its impact on both the welding process itself and the properties of the welded components. To simulate some of the most challenging degradation conditions, 1.5 mm thick electro-galvanized steel sheets were selected as the welding material DX51D+Zn275. For this type of material, the zinc coating tends to react with the electrode material during welding, forming a Zn-enriched layer, which accelerates electrode degradation. The experiments were conducted using an ELMA-Tech GmbH resistance spot welder. Short welding times were applied, with process parameters set at 70 ms, 12 kA, and an electrode pressing force of 2.5 kN. A total of 1100 welds were made under these conditions. Samples for mechanical testing and microstructural analysis were taken at 300, 500, and 1100 welds. A uniaxial tensile shear test was performed on the welded samples to determine the shear force at which failure occurred. Microscopic analysis was conducted using an optical microscope equipped for surface profiling and roughness measurements. Additionally, a scanning electron microscope (SEM) was used to analyze the electrodes after the welding process. Initial electrode roughness, measured as Rz = 1978.73 µm and Ra = 576.31 µm, displayed progressive wear and surface contamination, including zinc and burnt oil deposits that altered contact geometry, affecting electrode longevity. Roughness parameters evolved with weld counts and electrode wear correlated strongly with shear force. Chemical analyses have revealed the formation of a Zn-enriched layer and micro-cracking in electrodes, necessitating corrective machining after 1,100 welds to restore efficiency. These findings underscore the importance of managing electrode degradation to maintain weld quality and optimize industrial welding processes.

Keywords: high-frequency welding (HFW), spot welding, steel, properties, electrode degradation.

INTRODUCTION

The industry strives to improve the efficiency of technological processes. One of the most straightforward and effective strategies to achieve this is by reducing production time. This often involves optimizing existing machinery or integrating new technologies into processes. In the context of heat treatment for metal components, large-scale adoption of induction heating is being implemented, which enables rapid attainment of high temperatures. A similar trend is observed in metal joining for example through resistance spot-welding, where power sources with increased current frequency are increasingly employed – high-frequency electric resistance welding (HF ERW) [1, 2]. In both cases, the properties of the parts can be much better compared to classical methods, if the process is well understood and controlled. The development of spot-welding technology utilizing

high-frequency power sources has emerged in response to increasing industrial demands for improved efficiency and quality in material joining processes [3–7]. The use of higher frequency currents (in the range of several kHz) allows for more precise control of welding parameters, resulting in enhanced thermal stability and reduced time required to achieve optimal joining conditions. Studies have shown that high-frequency power sources contribute to improved weld consistency and mechanical properties compared to traditional low-frequency methods [8–10]. According to research by [11, 12], high-frequency spot welding reduces electrode wear and enhances the overall durability of the welded joints, making it a promising approach for advanced manufacturing applications, particularly in the automotive and aerospace industries. Moreover, these advancements allow for better control overheat distribution, minimizing the heat-affected zone (HAZ), and thereby improving the quality of welded assemblies [13–16].

High-frequency resistance welding (HFRW) achieves metal coalescence by generating heat through the resistance of workpieces to a high-frequency alternating current, typically above the standard 50 Hz, generally ranging from 50 kHz to 400 kHz in HFRW [8, 9, 17]. Following heating, an upsetting force is rapidly applied to complete the weld. The proximity effect controls the current flow within the workpiece, concentrating the heat in the welding zone. A key advantage of HFRW is that only a small volume of metal at the weld interface is heated, allowing for high-speed weld production with exceptional energy efficiency. The heat generated in the weld zone is predominantly influenced by the magnitude of the welding current, with even minor increases in the current significantly enhancing weld diameter, penetration, and strength. On most resistance welding machines, the welding current is regulated as a percentage of the equipment's rated power, though in some systems, adjustments are made by altering the gear ratio of the welding transformer. These adjustments allow for precise control of the welding process, enabling customization based on specific material and process requirements. Increasing the welding time (or current duration) alongside the welding current results in larger welds. Welding time is typically measured in cycles, with one cycle lasting 0.02 seconds at a power frequency of 50 Hz. The total energy input to the weld is thus a function of both the welding current and the duration of the welding time. Resistance welding is particularly suited for processes with short cycle times, favoring higher welding currents. Shorter welding times reduce heat dissipation to the surrounding areas, facilitating faster cooling and hardening of the weld. However, inadequate welding current can result in excessive heat being removed from the joining surface, leading to the formation of a weld pool. Conversely, excessively long welding times can increase electrode wear and create dents in the material, while also allowing heat to spread into a broader area, extending cooling times. Longer cooling periods can be advantageous when welding materials prone to brittleness or hardening, provided that sufficient hold time is maintained to ensure weld integrity.

Electrode wear in spot-welding is influenced by several key factors, including material properties, process parameters, and environmental conditions [17–25]. One of the primary causes of electrode degradation is the interaction between the electrode material and the workpiece, particularly when welding coated steels, such as galvanized sheets [26–28]. The zinc coating, for example, reacts with copper electrodes, forming a Zn-enriched layer (brass) at the interface, which accelerates wear and reduces the electrode's lifespan. Additionally, high welding currents, long weld times, and excessive electrode force contribute to increased thermal and mechanical stresses on the electrodes, leading to deformation, cracking, and material loss [18, 29, 30]. Studies by [22, 31–33] highlight that electrode wear is significantly accelerated in high-temperature conditions, where metal diffusion and surface oxidation play a crucial role. Moreover, the surface roughness and shape of the electrodes evolve during the welding process, altering the contact area and, consequently, the quality of the weld. These factors, combined with the cyclical nature of the welding process, result in gradual degradation of electrode performance, requiring frequent maintenance or replacement to ensure consistent weld quality [33, 34].

The specific resistance and transfer resistance of the zinc coating are lower than those of steel. The zinc coating may increase the influence of stray currents during resistance welding [17, 28, 31, 32]. Welding galvanized sheets requires longer welding times (by about 20–50%), greater force (by about 10–25%) and higher welding current (by about 30–40%) compared to welding uncoated steel. The purpose of resistance welding of coated materials is to allow the parent metals to join by giving way to the coating while keeping

the coating layer between the electrodes and the workpiece intact. To avoid zinc inclusions in the molten metal, the zinc coating must completely melt between the joined sheets. However, excessive heat input can also cause the zinc coating on the electrode contact surface to melt. In this case, the zinc coating on the finished product may be damaged and molten zinc may remain on the electrode tips, shortening their service life. The specific and contact resistances of the zinc coating are lower than those of steel, which can increase the influence of stray currents during resistance welding. Welding galvanized sheets requires extended welding times (approximately 20–50% longer), increased electrode force (by about 10–25%), and higher welding currents (by 30–40%) compared to uncoated steel [5]. The objective in resistance welding of coated materials is to ensure the base metals fuse while allowing the coating to be displaced, maintaining the integrity of the coating between the electrodes and the workpiece. To prevent zinc inclusions in the molten weld metal, the zinc coating must fully melt between the sheets being joined. However, excessive heat input can lead to the melting of the zinc coating at the electrode contact surface. In such cases, the zinc coating on the finished product may be compromised, and molten zinc can accumulate on the electrode tips, reducing their operational lifespan.

The objective of this study is to investigate how the cumulative number of spot welds affects electrode wear and the associated material degradation mechanisms. By systematically analyzing changes in electrode geometry and properties over successive welding cycles, the research aims to elucidate the impact of thermal and mechanical stresses on electrode longevity and performance. The findings are intended to provide insights that can inform the optimization of spot welding parameters, thereby enhancing operational efficiency and extending electrode lifespan.

MATERIALS AND METHODS

The electrode wear studies were conducted using the resistance spot welding method. The experiments utilized a resistance spot welder from ELMA-Tech GmbH (Figure 1) and were performed on steel sheets coated with zinc. The complete MIDIspot Vision AV system with individual components, includes flexible modular system, quick-release coupling element, high welding currents, high output currents up to 13 kA digital control with quality monitoring system, precision process and energy control parallel resistance detection. The selected sheet thickness was 1.5 mm in the grade DX51D+Zn275, with the zinc coating thickness ranging from 22 µm to 25 µm. The test material was not specifically manufactured for the research but was commercially purchased from Polish suppliers. This approach was taken to assess electrode wear on materials that are commonly used in commercial production of

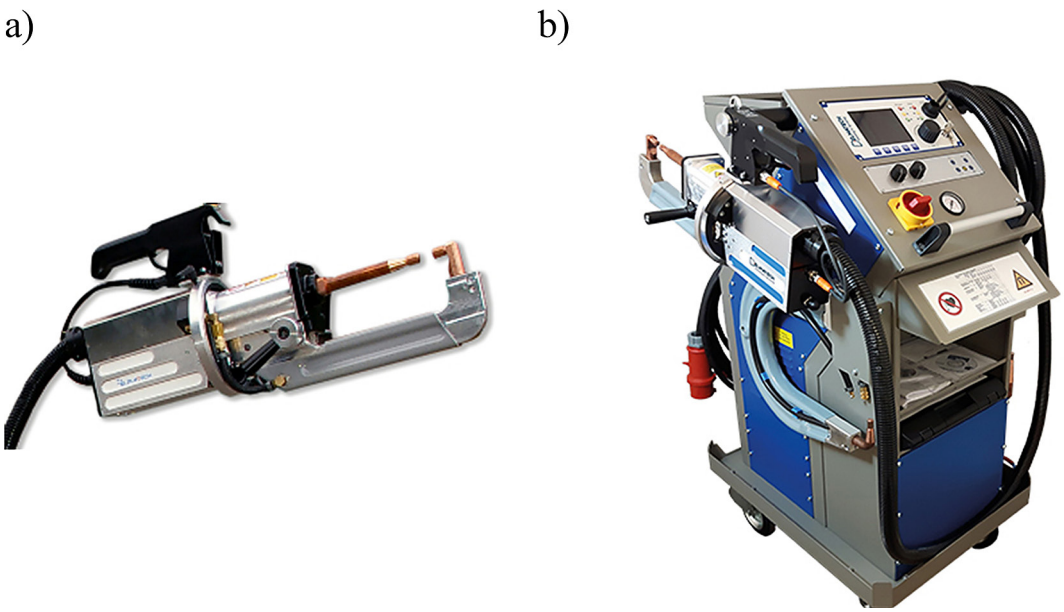

Figure 1. Test setup with the ELMA-Tech GmbH resistance spot welder MIDIspot Vision AV, (a) view of the welding head with electrodes and (b) overview of the complete system with individual components

welded components in numerous Polish factories. Similarly, a commercially available copper alloy with small additions of chromium and zirconium, Wirbalit HF (CuCr1Zr), was used, specifically designed for electrode production.

This study focused on the wear of flat electrodes. In our study, we utilized flat-type female spot welding electrode caps, classified as Type B (FB) according to ISO 5821:2009 standards. These electrode caps feature a female taper connection, designed to fit securely onto the electrode adaptor, ensuring consistent and reliable performance during resistance spot welding operations. The flat design of the electrode face is particularly suited for applications requiring uniform pressure distribution and minimal indentation on the workpiece. Adhering to the specified dimensions and tolerances outlined in ISO 5821:2009 ensures compatibility with standardized welding equipment and contributes to the reproducibility and accuracy of our experimental results. To ensure good electrode coaxiality, machining operations were performed, as misalignment could lead to uneven and accelerated wear. Before testing, the electrodes were cleaned and polished. Preliminary stereological studies were conducted to assess the surface quality of the electrodes using a scanning electron microscope (SEM) (Figure 2). A typical set of welding parameters was chosen for the tests, including a weld time of 70 ms, a current of 12 kA, and a clamping force of 2.5 kN. These parameters were recommended by the

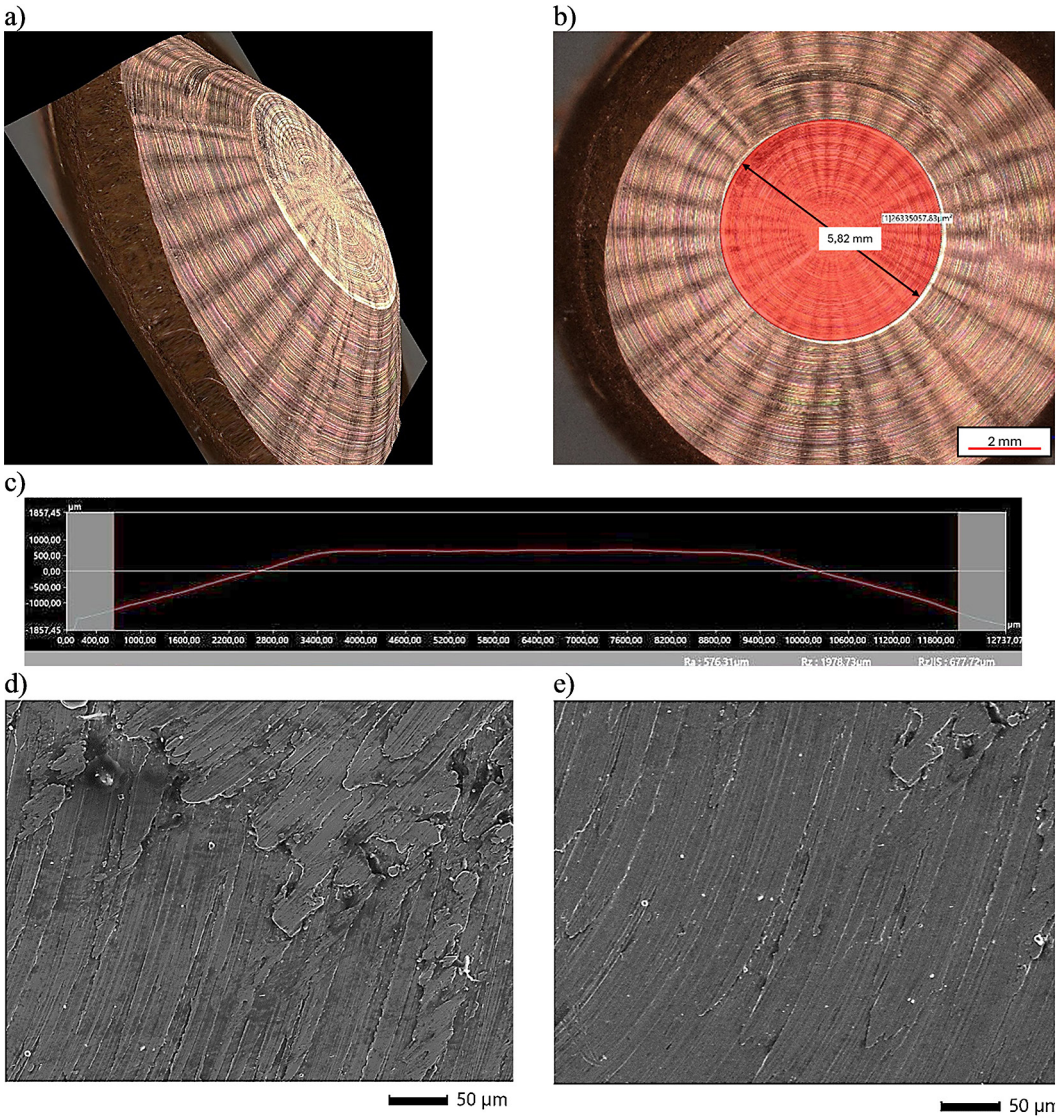

Figure 2. Results for the electrode before conducting the planned tests: (a) digital reconstruction of the side surface, (b) front surface, light microscope, (c) surface roughness profile, (d, e) front surface of the electrode, scanning electron microscope (SEM)

welder manufacturer to minimize zinc adhesion during welding of the sheets while ensuring satisfactory joint properties.

A total of 1100 welds were planned and completed on the described material using the selected parameters. During the welding process, three control points were chosen – at 300, 500, and 1100 welds – at which detailed metallurgical analyses of the welds and electrode wear assessments were conducted. Samples from the welded sheets were analysed for weld quality, including weld width and roughness, the resulting microstructure, and shear resistance in static tensile tests. For the electrodes, stereological studies were performed to evaluate changes in electrode shape profile and surface roughness. The obtained results provided valuable insights into the changes occurring in the electrodes during welding and their impact on the properties of the welded joints.

To ensure reliable results, the welding clamps were securely mounted on the table, while the sheet metal served as the movable component, slid on mounted supports to maintain consistent distances relative to the electrodes. This setup also allowed the sheet to be moved by the same distance for each weld. As a result, none of the welds overlapped with the preceding one (Figure 3a). As described, after a selected number of welds, several samples were cut from the sheet to evaluate the quality of the joints. Analysing the results for the initial state of the electrode (Figure 2), it can be concluded that the surface quality is comparable to typical electrodes used in industry. The working diameter of the electrode, representing the direct contact area with the material, measured 5.727 mm. The surface roughness parameters were Rz = 1978.73 µm and Ra = 576.31 µm. SEM observations revealed that no significant defects or discontinuities were observed in the electrode material.

RESULTS AND DISCUSSION

Figure 4 presents images of the electrode surface after completing the initially planned number of welds. For each interval, the width of the electrode's contact surface with the material was measured, and roughness measurements were taken, assessing the Ra and Rz parameters. Specifically, these parameters are defined as Ra – the arithmetic average of the absolute values of the profile height deviations from the centreline, and Rz – the vertical distance from the highest peak to the lowest valley within the scanned profile. Beneath the images of the electrode surfaces, a roughness profile across the electrode diameter is provided. This analysis allows for a precise

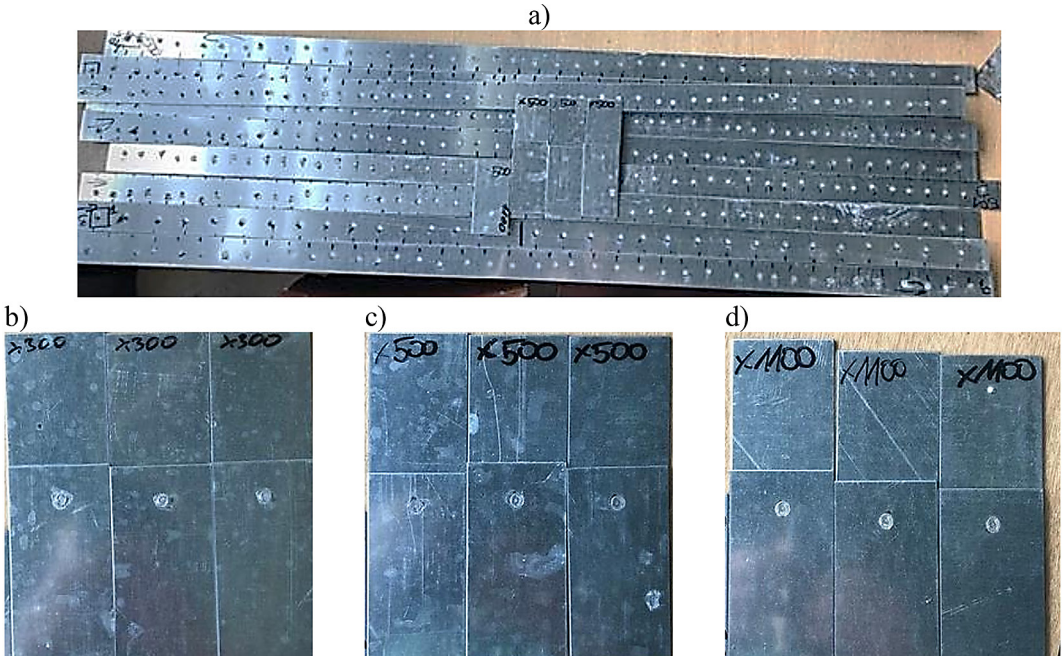

Figure 3. Macroscopic images of the sheet metal strips used in the study, illustrating the number of spot welds performed: (a) view of the initial 500 spot welds, with samples extracted for testing after: (b) 300 welds, (c) 500 welds, and (d) 1100 welds

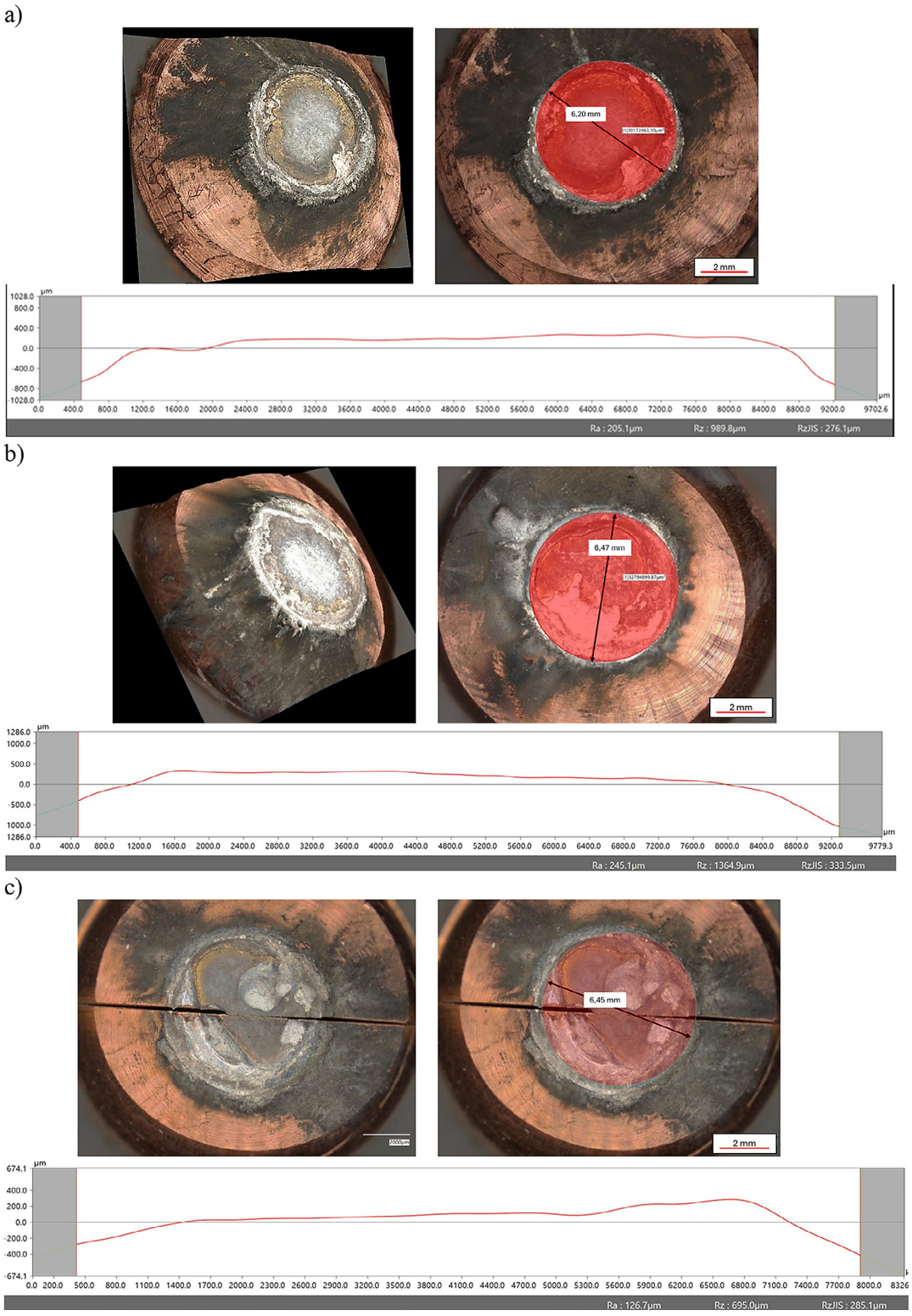

Figure 4. Macroscopic image of the electrode after (a) 300, (b) 500 and (c) 1100 welds with their roughness profiles

tracking of electrode degradation relative to the number of welds performed. Figure 5 displays images of the welds obtained after reaching the planned welding counts. Similar to the investigation of the electrodes, the widths of the welds and roughness parameters at the electrode-to-material contact points were measured. The obtained results are presented in the graphs in Figure 6, with a trend line fitted based on the linear regression coefficient R^2.

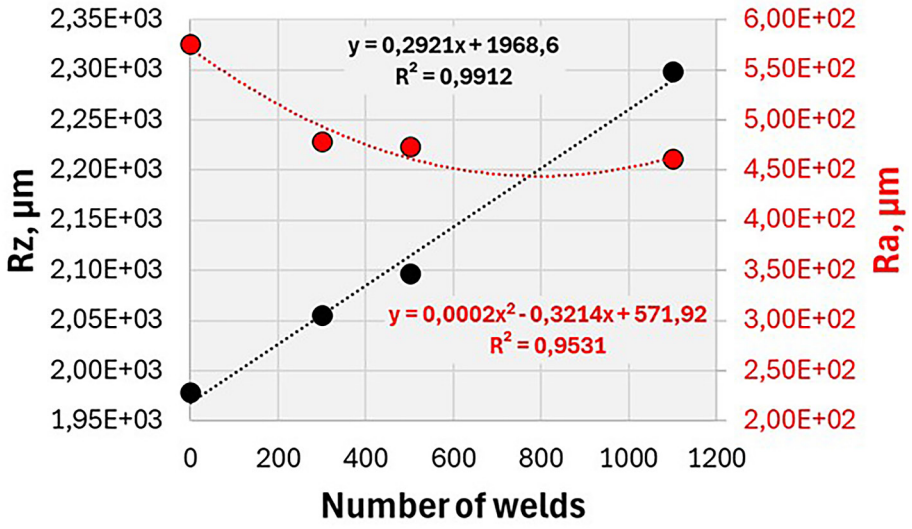

Figure 5. Changes in the Ra and Rz roughness parameters of the tested electrode as a function of the number of welds performed

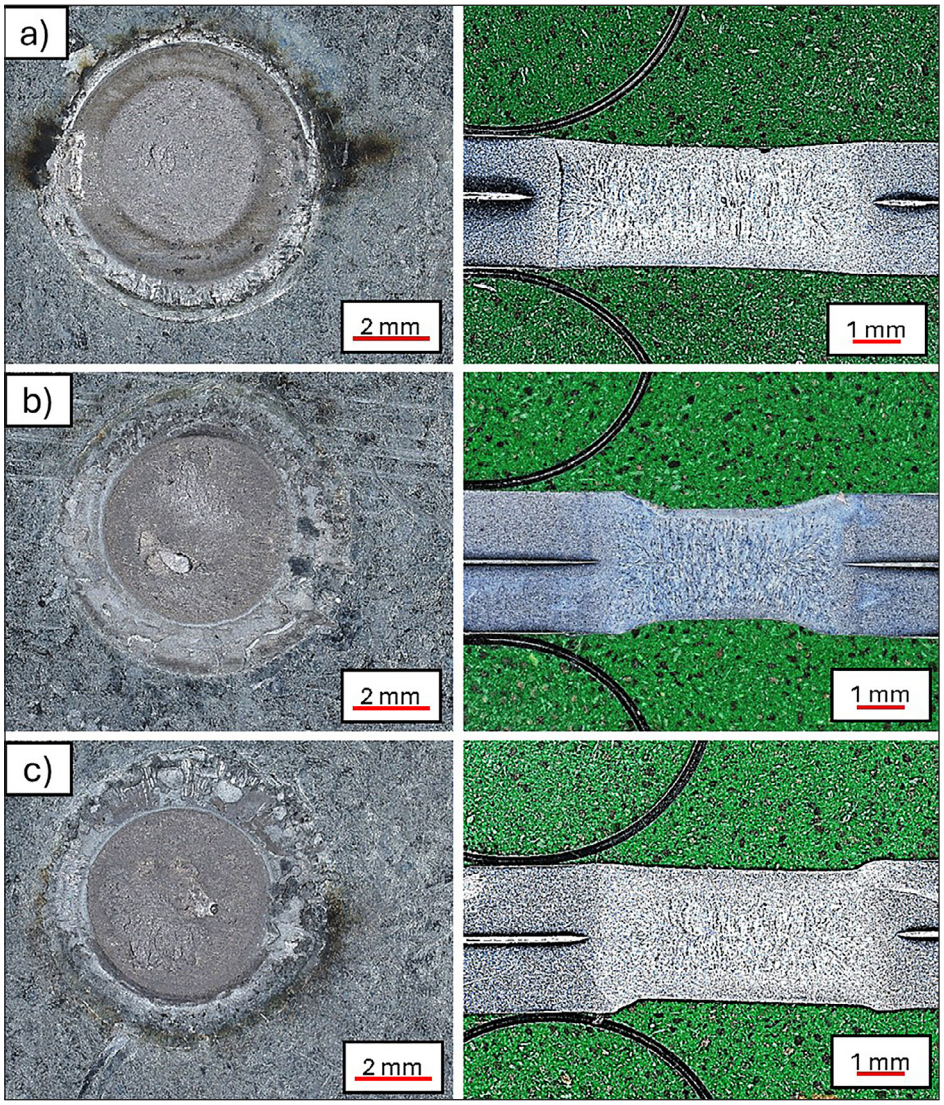

Figure 6. Images of the weld surface and its cross-section (weld nugget) after previously performing with the electrode (a) 300, (b) 500, and (c) 1100 welds

In each case, regardless of the number of welds performed, significant differences from the initial electrode surface condition can be observed. Each image reveals a black deposit, likely a result of burned contaminants (especially oils or other lubricants) at the contact interface between the welded material (sheet metal) and the electrode. The amount of this residue increases with the number of welds. Additionally, bright and grey areas are visible, which may correspond to zinc residues from the welding process and a Zn-enriched layer formation. The thickness and size of these areas grow proportionally with the number of welds. This accumulation of material significantly alters the contact surface geometry of the electrode. The observed changes at the electrode's contact surface have a direct impact on its roughness profile, as reflected in the measured Ra and Rz parameters (Figure 5). Surface irregularities can act as stress concentration points, which can affect the strength of the electrodes. Moreover, high roughness may affect heat transfer processes. The Rz parameter shows a linear increase with the number of welds, indicating that the electrode's surface exhibits greater height differences between the highest and lowest points. This may be due to zinc accumulation along the contact edge or the emergence of cracks. Interestingly, the Ra parameter displays a downward trend, best approximated by a quadratic function, with a possible minimum that may start to rise gradually. Considering these two parameters, it is suggested that the observed increase in Rz is primarily due to localized buildup along the edge in contact with the welded material, while the center of the electrode, interacting with the arc, partially reduces initial roughness, possibly due to zinc deposits. Beyond a certain number of welds, surface defects expand, developing into larger cracks. From a welding process repeatability perspective, this effect (despite the Ra decrease) is unfavourable. Localized changes in electrode height directly affect the microstructure of the weld and its properties. In extreme cases, insufficient material bonding in the weld may occur. After performing 1100 welds, a significant crack is visible on the electrode surface, although its initiation was not recorded during the process. This defect severely impacts process repeatability, and removal is only possible through machining (Figure 7).

The analysis of the performed welds on the sheets allowed us to trace how the described changes in the electrode impacted the surface quality of the obtained joints. In each case, apart from the contact area of the electrode with the welded material, a zone approximately 1 mm wide was identified in which deformations in the zinc coating were observed. This is naturally related to the applied force and the welding process itself. The roughness parameters of the weld, Rz and Ra, demonstrated similar behaviour depending on the number of performed welds. A logarithmic function was found to provide the best fit to these changes, with Ra showing a lower fit accuracy than Rz. This discrepancy may suggest that certain variables in the process affected the surface quality, or that the Ra parameter measurement was influenced by the evolving surface. The

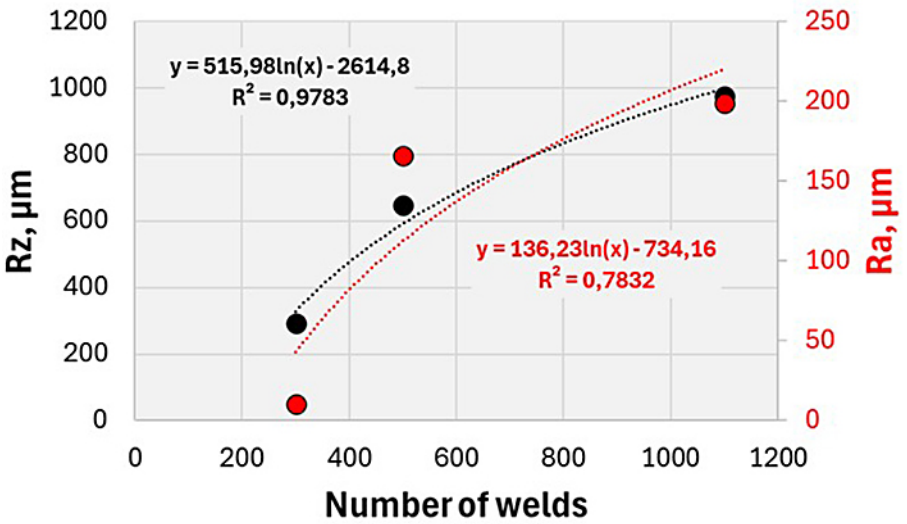

Figure 7. Changes in the Ra and Rz roughness parameters of the welded sheets as a function of the number of welds performed

logarithmic nature of these changes indicates a potential stabilization in the roughness parameter variation, although at relatively high values. Figure 8 presents a changes in the electrode diameter and the obtained welds as a function of the number of performed connections.

For the obtained results, regarding diameter changes in both the electrode and the weld, a logarithmic function provided the best fit. In the case of the electrode data, the fit was of a very high quality, while a notably poorer fit was observed for the weld diameter measurements. These results suggest that either a completely different factor has a significant influence on the weld diameter, or that the weld diameter measurements are affected by substantial error. In the first scenario, the changes in electrode diameter may induce notable variations in the currents forming the weld. In the second scenario, the presence of a zinc coating may interfere with the accurate visualization of the weld formation. Additional cross-sectional measurements of the welds did not yield better fits, which suggests potential inconsistencies in the welded sheets. It is known from metallurgical practice that the thickness of the zinc coating on galvanized sheets can vary along their length, and unfortunately, we cannot be certain that the purchased sheets were from the same production batch. In summary, the identified logarithmic dependencies indicate that the most significant diameter changes occurred in the initial phase of the process. After exceeding 1.100 welds, the observed changes diminish, and the function approaches a local maximum. This is likely due to the maximum diameter of the rod used to manufacture the electrode, increasing the direct contact area with the welded material. These observed changes are expected to have a substantial impact on the mechanical properties of the resulting joints.

In the next part of the study, tests were performed on a tensile testing machine for static uniaxial shear. The shear test of welded joints was conducted to assess the strength and mechanical properties of the welds under compressive forces, i.e., forces that act parallel to the material surface and attempt to displace one layer of material relative to another. The result of this test is a stress-strain curve, presented in Figure 9.

The recorded shear test curves for each sample are quite similar. After surpassing a force of approximately 2 kN, a change in the slope of the recorded force-displacement relationship is observed, likely indicating that the yield strength of the tested samples has been exceeded. A comparison of the recorded curves shows that the sample welded after using the electrode for 1100 welds achieved the highest shear strength, while the sample after 300 welds reached the lowest. Additionally, the largest deformation was also recorded for the sample welded after the highest number of welds. Notably, no catastrophic material failure occurred in any of the cases, suggesting that the weld nugget and individual zones, such as the heat-affected zone and the contact zone between the material and electrode, provided weld properties with high plasticity, likely due to grain refinement. The observed increase in

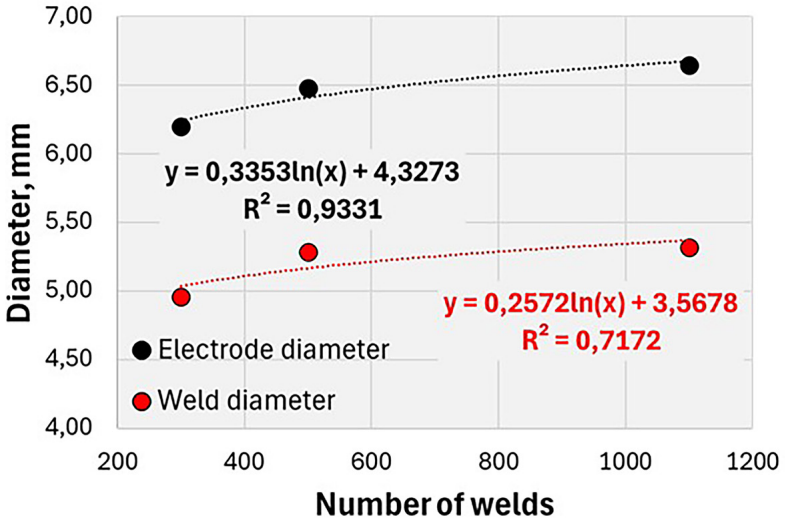

Figure 8. The changes in the electrode diameter and the obtained welds as a function of the number of performed connections

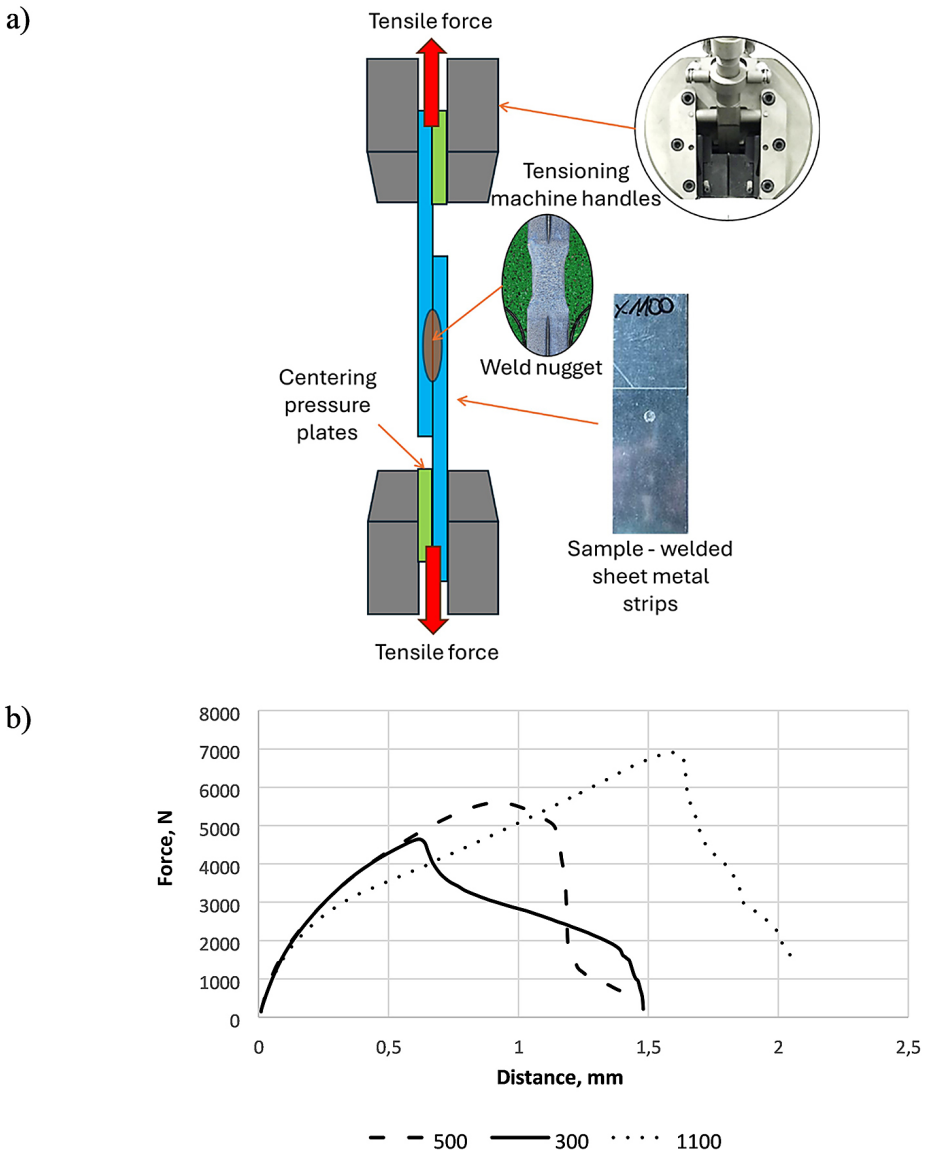

Figure 9. Results from the shear test (a) diagram of the sample layout in the machine, (b) results for selected samples

maximum shear forces is likely directly related to the previously described changes in electrode diameter and its impact on the resulting weld geometry. To determine the main factors influencing the observed weld properties, a basic analysis of individual parameters was conducted. Results were compared by plotting relationships based on various identified parameters for both the electrode and the weld. In our study, we employed various regression models – including linear, logarithmic, and exponential – to analyze the relationships between the shear strength of welds and factors such as electrode roughness, changes in electrode diameter, number of welds performed, and weld diameter. The selection of the appropriate regression model for each analysis was based on the observed data distribution and the nature of the relationship between variables. Specifically, scatter plots were examined to assess linearity, and the model that best fit the data was applied, as indicated by higher coefficients of determination (R^2 values). This methodological approach aligns with standard practices in statistical analysis, ensuring that the selected model accurately represents the underlying data patterns. However, we acknowledge the limitation posed by the relatively small sample size, with analyses based on measurements taken after 300, 500, and 1,100 welds. While a larger number of data points would enhance the robustness of statistical inferences, the scope of our experimental setup constrained the frequency of measurements. It

is important to note that small sample sizes can lead to increased variability and reduced statistical power, potentially affecting the generalizability of the findings. Therefore, we emphasize the need for cautious interpretation of the results and suggest that future studies incorporate more frequent sampling to validate and extend our findings. Graphs showing high (above 0.60) and very strong correlations (above 0.85) are presented collectively in Figure 10.

From the presented graphs, the most significant factors influencing the properties of welded galvanized sheets identified in this study can be highlighted. Similar to the observed variation in weld diameter relative to the number of welds, the correlation of these results with the designated shear forces showed a weak functional fit (Figure 10a). This confirms that simply determining the diameter of the welds is insufficient to fully describe the changes occurring in the welded material as the number of welds increases. This suggests the need for further stereological studies to describe both the weld core and the shape and quality of the heat-affected zone. Additionally, metallurgical data focused on the microstructure of the welds may be required. Strength tests indicate the formation of a fine microstructure in the individual zones. To confirm this, a greater number of stereological and statistical microstructure analyses are needed. Due to the extensive results presented in this study, this topic will not be further developed here. The best fit was observed for the relationship between shear force and the number of welds, with an R^2 value of 0.998 (Figure 10e). As discussed previously, the function approaches a maximum, stabilizing significantly after approximately 10.000 welds. As shown in the study, the occurrence of cracking prevents achieving such a high number of welds with the

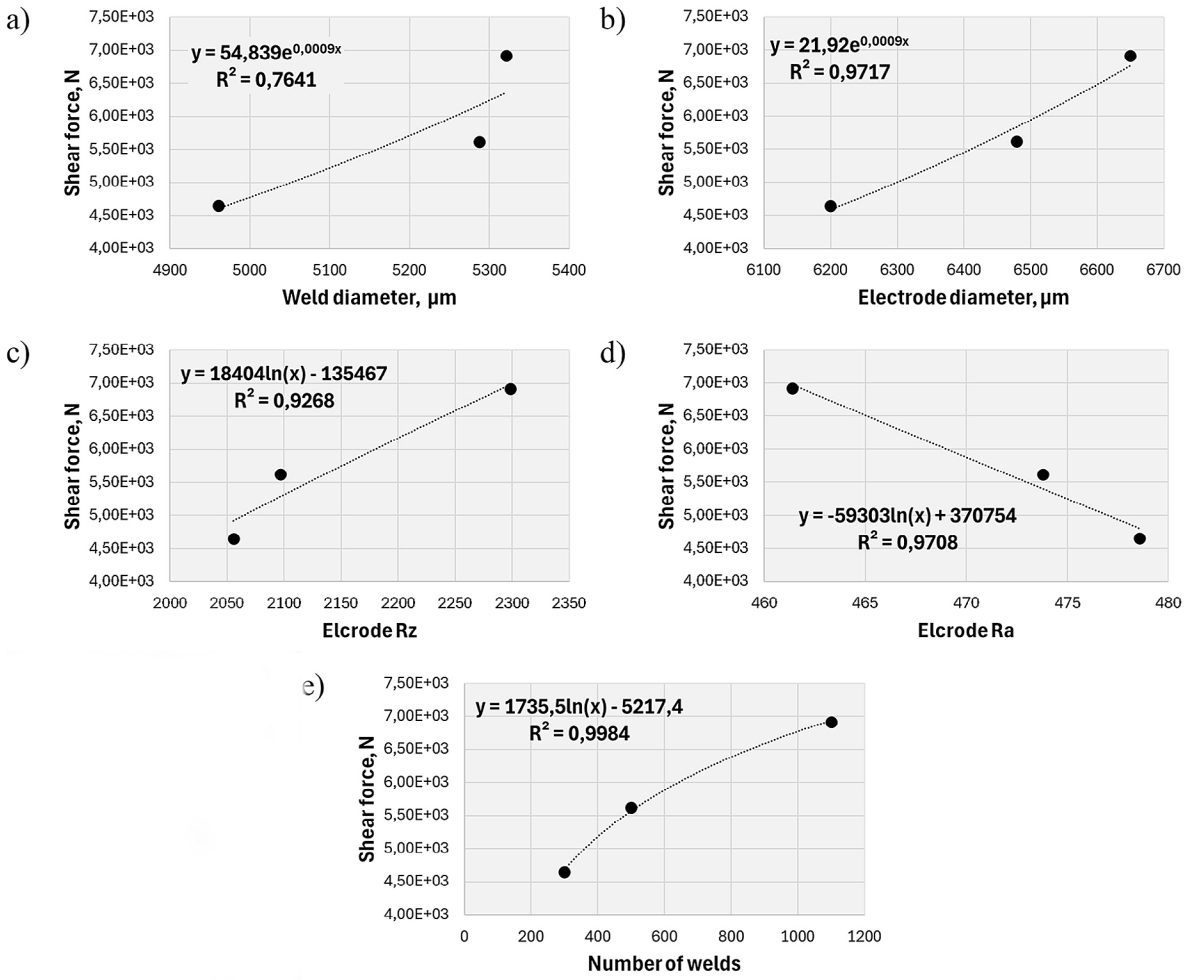

Figure 10. Graphs of plotted results based on various relationships (a) shear force (weld diameter), (b) shear force (electrode diameter), (c) shear force (electrode maximum height of the profile Rz), (d) shear force (electrode average roughness Ra) and (e) shear force (numbers of welds)

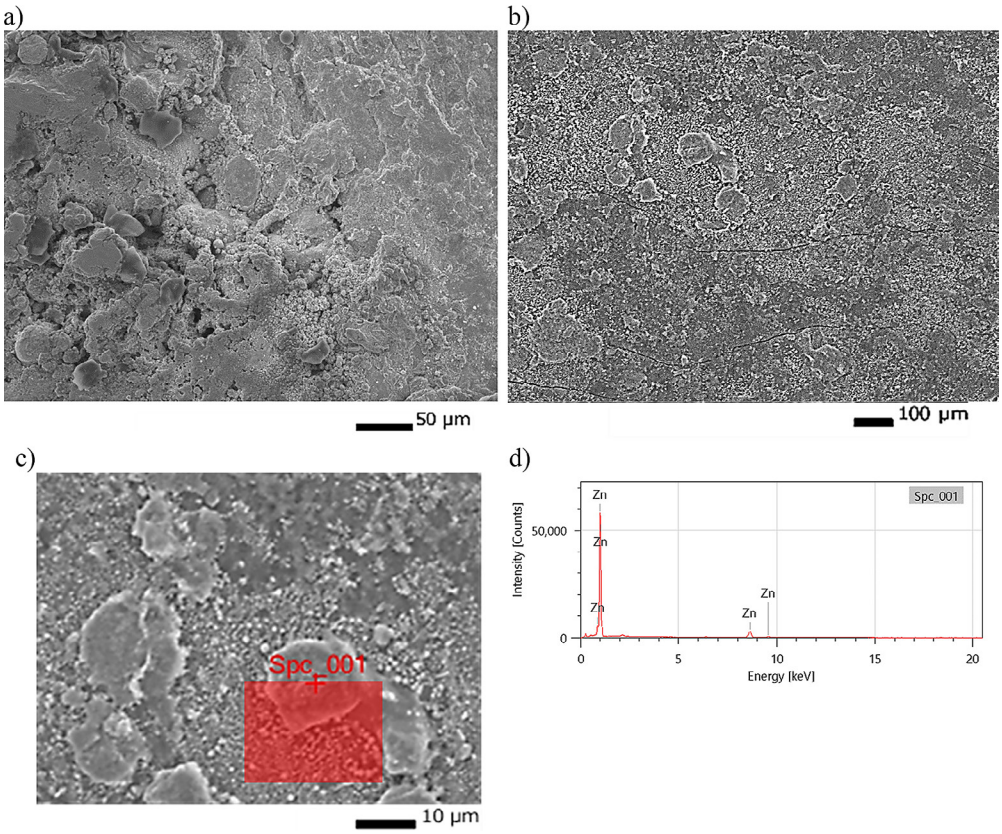

Figure 11. Surface of the electrode that made 300 welds with EDX analysis

chosen electrode material and technique. Similarly, the relationship between shear force and the working width of the electrode showed a high fit, with $R^2 = 0.972$ (Figure 10b). The absence of an equally strong correlation for weld width suggests that, as noted, electrode width has a greater influence on the resulting microstructure. The likely reduction in current density due to increased electrode width would result in lower temperatures in the weld area, leading to a finer microstructure.

When analysing changes in electrode surface roughness in relation to the number of welds and its influence on shear forces, a strong correlation was also confirmed for the Rz parameter ($R^2 = 0.927$, Figure 10c) and for the Ra parameter ($R^2 = 0.971$, Figure 10d). These findings confirm that the described changes in the electrode are key factors influencing weld properties. Variations in roughness may locally disturb the force field of the welding currents, creating a type of gradient microstructure dependent on the quality of the electrode's contact with the welded material. These relationships prompted a detailed analysis of the electrode surface using SEM and EDX analysis. The results, including images of the electrode surface and selected chemical composition analyses, are presented in Figures 11–13. According to literature reports, chemical composition analyses confirmed the reaction between the zinc coating and the electrode material. Interestingly, for the electrode tested after 300 welds, zinc presence was highly localized, forming somewhat spheroidal deposits on the surface. As the number of welds increases, zinc begins to occupy a progressively larger surface area. Observations suggest that Zn-enriched layer formation occurs. The chemical composition analysis of the electrode surface after 1100 welds reveals the presence of more complex phases involving additional elements, such as Mn and Cr. High-magnification surface observations reveal the appearance of microcracks at the initial stages. After 500 welds, no further cracking was observed, likely due to the interaction with the zinc coating on the sheet metal. Zinc may fill in the initially formed microcracks. For the electrode surface after 1100 welds, a significant morphological change is evident. Several areas display visible deposits, which may be regions of formed Zn-enriched layer. Due to its differing coefficient of thermal expansion, this layer may have a tendency to crack and delaminate.

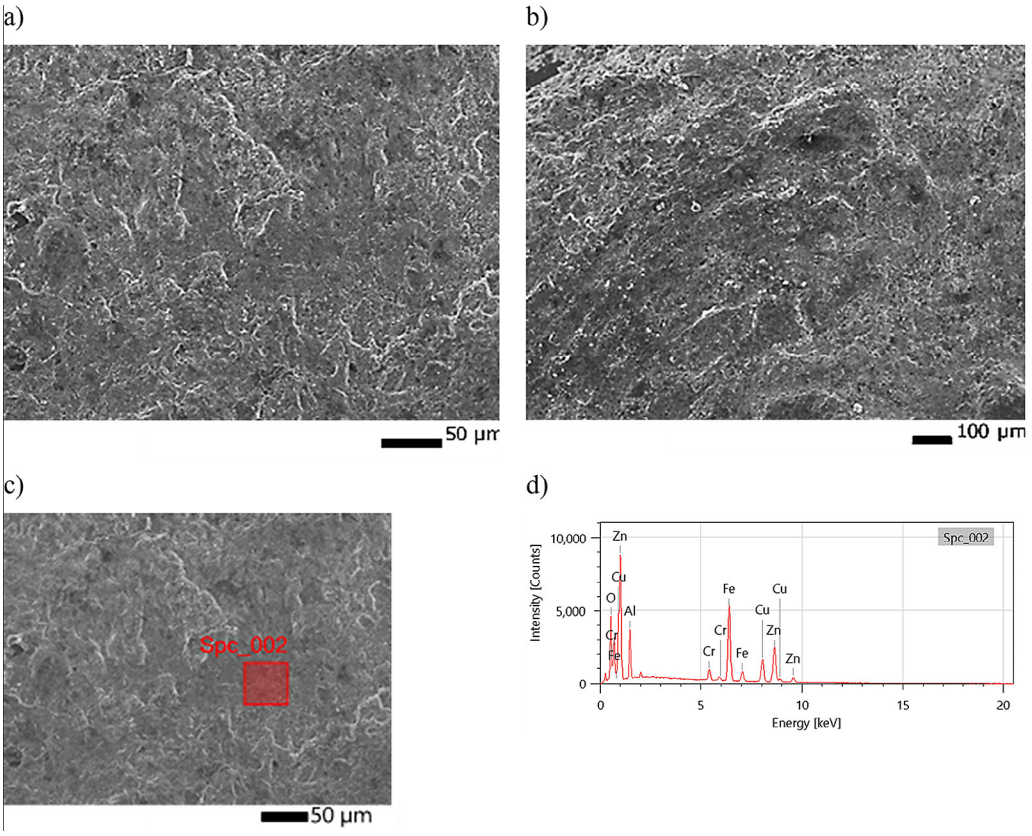

Figure 12. Surface of the electrode that made 500 welds with EDX analysis

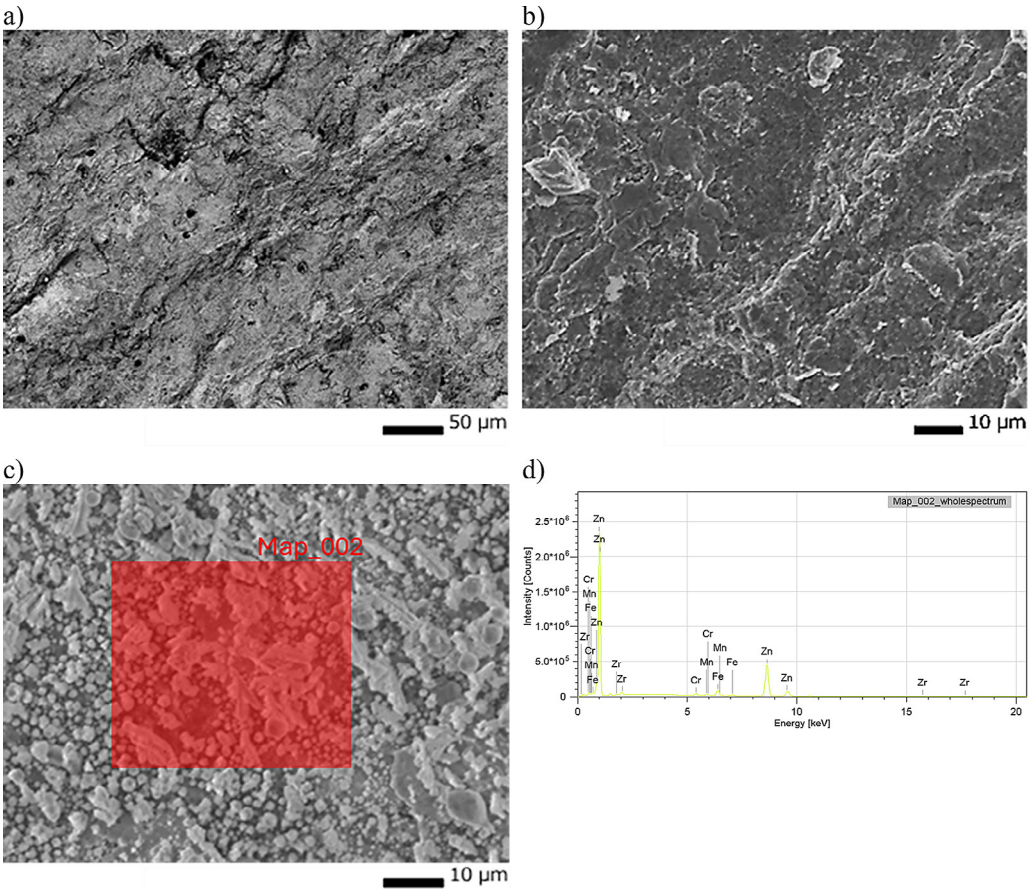

Figure 13. Surface of the electrode that made 1 100 welds with EDX analysis

In summary, from the perspective of the joined sheets, performing 1100 welds improves the shear strength of the joints while maintaining similar weld quality. However, the final number of welds resulted in the appearance of a significant crack, which can only be removed through machining. Welding galvanized sheet metal presents specific challenges impacting electrode longevity. The electrodes can wear due to high electric currents and friction, leading to reduced weld quality and joint durability. Precise control of welding parameters – current, pressure, welding time, and electrode geometry – is essential for achieving high-quality, durable welds. Poorly optimized settings can degrade both electrode lifespan and weld integrity. Continuous monitoring of joint quality and process adjustment during successive welds are critical to maintaining weld reliability. Regular electrode maintenance, including cleaning, sharpening, and zinc deposit removal, helps preserve electrode geometry and mechanical performance.

CONCLUSIONS

Based on the conducted research and analysis of the results, the following key conclusions can be formulated:

a) stability and quality of welds: the consistent placement of the welding head and stable positioning of the metal sheets ensured repeatable weld quality without overlap, allowing precise assessment of weld consistency and minimizing variability in the electrode's contact area with the material;
b) surface roughness and electrode wear: Initial analysis of the electrode's surface showed surface roughness parameters Rz = 1978.73 µm and Ra = 576.31 µm. SEM observations indicated wear mechanisms such as plastic deformation and micro-scratching, leading to noticeable material deposits on the electrode surface, yet no significant defects were detected;
c) progressive surface contamination: a noticeable increase in surface contamination, observed as black residue and zinc deposits, occurred with increasing weld counts. This contamination, likely originating from burned oils or zinc residuals, significantly altered the geometry of the electrode-material interface, impacting subsequent welds and the electrode's wear rate.
d) roughness parameters and degradation: the Rz parameter increased linearly with the number of welds, suggesting localized roughness peaks due to zinc deposits or micro-cracking. Conversely, Ra showed a non-linear trend, initially decreasing before a gradual rise, likely due to localized zinc adhesion in the electrode's contact area;
e) impact on weld properties: changes in electrode diameter and weld diameter displayed a logarithmic trend with increasing weld counts, stabilizing after approximately 10,000 welds. This trend suggests that electrode surface wear and contamination gradually stabilize at high counts, potentially due to a balance between deposit buildup and mechanical abrasion;
f) shear strength correlation – mechanical testing revealed a high correlation (R^2 = 0.998) between the number of welds and shear strength, indicating that electrode wear significantly impacts joint strength. The strongest welds were achieved at higher weld counts, with plastic deformation evident at high shear loads, confirming the durability and quality of joints under compressive forces;
g) energy dispersive spectroscopy (EDS) analyses conducted after 300, 500, and 1,100 resistance spot welds reveal a progressive increase in zinc concentration on the electrode surfaces. This trend suggests the formation of a zinc-enriched layer, which, under welding temperatures, may facilitate localized brass (copper-zinc alloy) formation at the electrode interface. Such alloying can adversely affect electrode longevity and weld quality, as corroborated by existing literature. Therefore, implementing strategies to mitigate zinc accumulation is essential to enhance electrode performance and ensure consistent weld integrity. Increasing welds, led to more complex chemical compositions and morphological changes, including microcracking. After approximately 1,100 welds, significant morphological alterations in the electrode surface required corrective machining to restore functionality.

These findings highlight the intricate relationship between electrode surface evolution, material contamination, and the mechanical integrity of welds. The results suggest that understanding and managing electrode degradation are crucial for ensuring weld quality and optimizing industrial welding processes.

Acknowledgement

The research was carried out as part of the project titled AWTech - Innovative Solutions in the Area of Frame Welding, co-financed by the European Union from the European Regional Development Fund under the Smart Growth Operational Programme 2014–2020. The project was implemented as part of the National Centre for Research and Development competition: Fast Track. Research project partly supported by program „Excellence initiative – research university" for the AGH University.

REFERENCES

1. Schmidt M., Spieth H., Haubach C., Kühne C. Resistance spot welding made easy, in: 100 Pioneers in Efficient Resource Management, 978th-3rd-662nd- ed., Springer Spektrum, Berlin, Heidelberg, Berlin, Heidelberg, 2019: pp. 438–441. https://doi.org/10.1007/978-3-662-56745-6_94
2. Shen Y., Xia Y.-J., Li H., Zhou L., Li Y.-B., Pan H.-T. A novel expulsion control strategy with abnormal condition adaptability for resistance spot welding, Journal of Manufacturing Science and Engineering 2021; 143. https://doi.org/10.1115/1.4051011
3. Pouranvari M., Marashi S.P.H. Critical review of automotive steels spot welding: process, structure and properties, Science and Technology of Welding and Joining 2013; 18: 361–403. https://doi.org/10.1179/1362171813Y.0000000120
4. Zhou K., Yao P. Overview of recent advances of process analysis and quality control in resistance spot welding, Mech Syst Signal Process 2019; 124: 170–198. https://doi.org/https://doi.org/10.1016/j.ymssp.2019.01.041
5. Raut M., Achwal V. Optimization of spot welding process parameters for maximum tensile shear strength, International Journal of Mechanical Engineering and Robotics Research 2014; 3: 506–517.
6. Hamidinejad S.M., Kolahan F., Kokabi A.H. The modeling and process analysis of resistance spot welding on galvanized steel sheets used in car body manufacturing, Mater Des 2012; 34: 759–767. https://doi.org/10.1016/j.matdes.2011.06.064
7. Kaščák Ľ., Cmorej D., Spišák E., Slota J. Joining the high-strength steel sheets used in car body production, Advances in Science and Technology Research Journal 2021; 15: 184–196. https://doi.org/10.12913/22998624/131739
8. Ravikiran K., Xu P., Li L. A critical review on high-frequency electric-resistance welding of steel linepipe, Journal of Manufacturing Processes 2024; 124: 753–777. https://doi.org/10.1016/j.jmapro.2024.06.046
9. Wagner M., Kolb S. Efficiency improvements for high frequency resistance spot welding, in: 2013 15th European Conference on Power Electronics and Applications (EPE), 2013; 1–9. https://doi.org/10.1109/EPE.2013.6634720
10. Aydin K., Hıdıroğlu M., Kahraman N. Enhancing weld strength in high-strength steels: the role of regional preheating in RSW, Materials Testing 2024; 66: 328–346. https://doi.org/doi:10.1515/mt-2023-0241
11. Mathiszik C., Köberlin D., Heilmann S., Zschetzsche J., Füssel U. General approach for inline electrode wear monitoring at resistance spot welding, Processes 2021; 9. https://doi.org/10.3390/pr9040685
12. Ahola A., Savolainen J., Brask L., Björk T. Fatigue enhancement of welded thin-walled tubular joints made of lean duplex steel, Journal of Constructional Steel Research 2024; 218. https://doi.org/10.1016/j.jcsr.2024.108738
13. Matsuyama K., Matsuyama K. Spot welding system and method for sensing welding conditions in real time, U.S. Patent No. 6,506,997, 2001.
14. Matsui K. Research on practical application of dual frequency induction hardening to gears, JSAE Review 1998; 19: 358–360. https://doi.org/10.1016/S0389-4304(98)00027-7
15. Senkara J., Zhang H., Hu S. Expulsion prediction in resistance spot welding, WELDING JOURNAL-NEW YORK 2004; 83: 123–125.
16. Williams N.T., Parker J.D. Review of resistance spot welding of steel sheets: Part 1 - Modelling and control of weld nugget formation, International Materials Reviews 2004; 49: 45–75. https://doi.org/10.1179/095066004225010523
17. Shome M., Chatterjee S. Effect of material properties on contact resistance and nugget size during spot welding of low carbon coated steels, ISIJ International 2009; 49: 1384–1391. https://doi.org/10.2355/isijinternational.49.1384
18. Başkaya Ü., Uzun R., Atapek H., Kılıç Y., Polat Ş. Effect of coating type on electrode degradation and its life in resistance spot welding of a low carbon steel, Eng Fail Anal 2024; 157. https://doi.org/10.1016/j.engfailanal.2023.107879
19. Simmons J.G. Electric tunnel effect between dissimilar electrodes separated by a thin insulating film, J Appl Phys 1963; 34: 2581–2590. https://doi.org/10.1063/1.1729774
20. Kogut L., Komvopoulos K. Analysis of interfacial adhesion based on electrical contact resistance measurements, J Appl Phys 2003; 94: 6386–6390. https://doi.org/10.1063/1.1618925

21. Feulvarch E., Robin V., Bergheau J.M. Resistance spot welding simulation: A general finite element formulation of electrothermal contact conditions, J Mater Process Technol 2004; 153–154: 436–441. https://doi.org/10.1016/j.jmatprotec.2004.04.096
22. Rogeon P., Carre P., Costa J., Sibilia G., Saindrenan G. Characterization of electrical contact conditions in spot welding assemblies, J Mater Process Technol 2008; 195: 117–124. https://doi.org/10.1016/j.jmatprotec.2007.04.127
23. Na S.J., Park S.W. A theoretical study of electrical and thermal response in resistance spot welding, 1996; 75.
24. Kahraman N. The influence of welding parameters on the joint strength of resistance spot-welded titanium sheets, Mater Des 2007; 28: 420–427. https://doi.org/10.1016/j.matdes.2005.09.010
25. Kubit A., Kłosowski G., Berezowski W. The use of artificial intelligence for quality assessment of refill friction stir spot welded thin joints, Advances in Science and Technology Research Journal 2024; 18: 45–57. https://doi.org/10.12913/22998624/185618
26. Wei P.S., Wang S.C., Lin M.S. Transport phenomena during resistance spot welding, Journal of Heat Transfer (1996) 118: 762–773. https://doi.org/10.1115/1.2822697.
27. M. Galler, N. Enzinger, C. Sommitsch, The estimation of the contact interface temperature during resistance spot welding of zinc coated steels using numerical technique, Material wissenschaft Und Werkstofftechnik 41 2010; 925–930. https://doi.org/10.1002/mawe.201000686
28. Gedeon S.A., Eagar T.W. Resistance spot welding of galvanized steel: Part I. Material variations and process modifications, Metallurgical Transactions B 1986; 17: 879–885. https://doi.org/10.1007/BF02657151
29. Bowers R., Sorensen C., Eagar T. Electrode geometry in resistance spot welding, Welding Journal 1990; 69: 45S.
30. Aslanlar S., Ogur A., Ozsarac U., Ilhan E. Welding time effect on mechanical properties of automotive sheets in electrical resistance spot welding, Materials and Design 2008; 29: 1427–1431. https://doi.org/10.1016/j.matdes.2007.09.004
31. Chan K.R. Weldability and Degradation Study of Coated Electrodes for Resistance Spot Welding, Waterloo, Ontario, Canada 2005; 1–120.
32. Howe P., Kelley S.C. A Comparison of the resistance spot weldability of bare, hot–dipped, galvannealed, and electrogalvanized DQSK sheet steels, SAE Transactions 1988; 97: 138–152.
33. Zhang Y.S., Wang H., Chen G.L., Zhang X.Q. Monitoring and intelligent control of electrode wear based on a measured electrode displacement curve in resistance spot welding, Measurement Science and Technology 2007; 18: 867–876. https://doi.org/10.1088/0957-0233/18/3/040
34. Ling S.F., Wan L.X., Wong Y.R., Li D.N. Input electrical impedance as quality monitoring signature for characterizing resistance spot welding, NDT and E International 2010; 43: 200–205. https://doi.org/10.1016/j.ndteint.2009.11.003